Ultrafast Carotenoid Band Shifts: Experiment and Theory†

J. L. Herek,[#] M. Wendling,[||] Z. He,[‡] T. Polívka,[‡] G. Garcia-Asua,[§] R. J. Cogdell,[⊥] C. N. Hunter,[§] R. van Grondelle,[||] V. Sundström,[‡] and T. Pullerits*[,‡]

Department of Chemical Physics, Lund University, P.O. Box 124, S-22100 Lund, Sweden, Krebs Institute and Robert Hill Institute for Photosynthesis, Department of Molecular Biology and Biotechnology, University of Sheffield, Western Bank, Sheffield S10 2TN, U. K., Division of Physics and Astronomy, Faculty of Sciences, Vrije Universiteit, de Boelelaan 1081, 1081 HV Amsterdam, The Netherlands, IBLS, University of Glasgow, Glasgow G12 8QQ, U. K., and FOM-Institute for Atomic and Molecular Physics, Kruislaan 407, 1098 SJ Amsterdam, The Netherlands

Received: February 4, 2004; In Final Form: May 14, 2004

The ultrafast carotenoid band shift upon excitation of nearby bacteriochlorophyll molecules was studied in three different light harvesting complexes from purple bacteria. The results were analyzed in terms of changes in local electric field of the carotenoids. Time dependent density functional theory calculations based on known and model structures led to good agreement with experimental results, strongly suggesting that the mutual orientation of the pigment molecules rather than the type of the carotenoid molecules determines the extent of the ultrafast band shift. We further estimate that the protein induced local field nearby carotenoid molecule is about 4 or 6 MV/cm, depending on the orientation of the change of the electrical dipole in the carotenoid upon optical transition.

Introduction

Carotenoids (Car) have a wide range of roles in nature. In photosynthetic antenna systems they have two major functions: photoprotection and light harvesting.[1,2] In some antennas they also serve a structural role.[3] Electronic level structure and ultrafast photophysical processes in Car molecules have become a hot topic in photosynthesis research. This interest has been largely stimulated by availability of high quality structural information with Car molecules clearly resolved.[4,5]

One of these structures, the peripheral light harvesting complex (LH2) of purple bacteria consists of two concentric rings of BChl molecules named B800 and B850 according to their characteristic Q_y absorption maxima at 800 and 850 nm. The BChls of B800 are well-separated from each other and from B850s and thereby have mainly monomeric spectroscopic properties. Contrary to that, the B850 ring forms a rather densely packed excitonically coupled aggregate with partially delocalized excited states. The Car molecules in LH2 "snake" between the two BChl rings. Excitation absorbed in the B800 ring is transferred to the B850 ring with a time constant of 0.7 ps at room temperature.[6,7] The transfer slows down at low temperatures.[8] It has been argued that the Car molecule can be involved in facilitating the B800 to B850 transfer,[9] whereas in more recent models the coupling of the B800 with nearly resonant B850 exciton levels, which have negligible transition dipole moment, seems to lead to a quantitative agreement between theory and experiment.[10,11] Also the generalized master equation approach has been recently successfully applied. [12]

Electronic states of Car molecules are usually assigned in terms of the C_{2h} point symmetry group. Even though the Car molecules' C_{2h} symmetry is not perfect, the assignment enables understanding of many photophysical observations.[2] The main absorption of Car in the visible spectral region is due to the transition from the ground-state S_0 ($1A_g$) to the second excited-state S_2 ($1B_u$). The lowest singlet excited-state S_1 ($2A_g$) has the same parity as the ground state and therefore has negligible one-photon absorption. The Pariser, Parr, and Pople (PPP) Hamiltonian of the polyene π-electron system gives rise to yet another approximate symmetry, a so-called Pariser alternancy symmetry,[13] leading to $\pm$ labels on top of the point symmetry notation. Based on these considerations a dark state identified in resonance Raman excitation profiles of spheroidene located between S_1 and S_2 states was assigned as a $1B_u$ state.[14] Interestingly, neither time dependent density functional theory (TDDFT)[15] nor complete active space (CAS)[16] calculations have found such a state. Recently a Car singlet state S* was assigned as a distinct precursor of the ultrafast singlet-to-triplet conversion process found in some antenna complexes.[17] The identity of that state is still not entirely clear.

In most photosynthetic systems antenna Car molecules efficiently transfer excitation energy to chlorophyll or BChl molecules. The transfer occurs from both the S_2 and S_1 states.[18,19] The transfer from S_2 is well understood in terms of the Förster mechanism.[20] Since S_1 does not have any transition dipole moment, the transfer mechanism from that state has been heavily debated.[2] Already Nagae et al. concluded that the quadrupole−dipole interaction is much larger than exchange interaction for that transfer step.[21] Transition quadrupole can be seen as a first refinement of the transition dipole in calculating the Coulomb coupling. A so-called transition density cube method[22] is in this context exact as long as the wave functions, which are used for constructing the transition densities, are correct. Recent transition density cube calculations based on

† Part of the special issue "Gerald Small Festschrift".
* Corresponding author.
‡ Lund University.
§ University of Sheffield.
|| Vrije Universiteit.
⊥ University of Glasgow.
FOM-Institute for Atomic and Molecular Physics.

10.1021/jp040094p CCC: $27.50
Published on Web 06/02/2004

TDDFT have led to quantitative agreement between experimental and calculated Car S_1 to BChl transfer rates.[15] It has been also pointed out that mixing of the S_1 with the S_2 state[15,23] or with the charge transfer state (CTS)[24] leads to appreciable fluorescing transition dipole of the S_1, which may open up the possibility for the conventional Förster transfer in some systems.

From all this it is clear that there are still many open questions about photoexcited states and their dynamics in Car molecules. In LH2, recent discovery of the second carotenoid site located at the periphery of the complex further complicates interpretation of Car−BChl energy transfer pathways.[25] In the current article we will address still another interesting phenomenon taking place in Cars: the ultrafast shift of the Car absorption band that occurs upon exciting BChl molecules of LH2. The effect was first observed in membranes of mutants of purple bacterium *Rhodobacter (Rb.) sphaeroides* containing neurosporene as the predominant Car.[26] It is known from various experiments that Car molecules have a strong electrochromic shift of the absorption band.[27] This effect, a so-called Stark shift, has been used to study the transmembrane potential of charge separation in photosynthetic membranes.[28] Also, the field of a photogenerated ion pair in an electron donor−acceptor system has been studied using Car Stark shift.[29] Along the same line, the above Car band shift in LH2[26] was interpreted as a Stark shift due to the changes in the local electric field near Car molecules upon photoexcitation of the BChl molecules. This interpretation was further supported by quantum chemical calculations.[16] In the present article we extend the Car band shift study to three other LH2 systems: (i) *Rhodopseudomonas (Rps.) acidophila* containing the rhodopin glucoside (RG) Car molecule, (ii) *Rhodospirillum (Rs.) molischianum* containing lycopene, and (iii) a mutant of *Rhodobacter (Rb.) sphaeroides* containing lycopene.

Materials and Methods

Samples. For *Rps. acidophila* and *Rsp. molischianum*, the LH2 complexes were extracted from membranes and purified according to established methodologies.[30] The stock solutions were maintained at −40 C until ready for use, at which point a small portion was dissolved in buffer solution (50 mM Tris, pH 8 and 0.1% LDAO) and diluted with ∼60% glycerol to ensure clear glass formation. The concentration was characterized by the room temperature absorption spectrum and carefully adjusted to OD (795 nm) = 0.5 in a 3 mm acrylic cuvette. Note that both the *Rps. acidophila* and *Rsp. molischianum* samples were prepared in the same manner and at the same time, and were loaded together in a stacked configuration into the cryostat. This allowed for a direct comparison of their spectral and dynamic behavior, with identical laboratory conditions. The temperature for these measurements was 77 K, and the excitation intensity (λ = 795 nm) was 140 μJ/pulse with a spot size of 400 μm. At this intensity, no singlet−singlet annihilation or sample degradation effects could be observed.

The third sample studied was a mutant of *Rb. sphaeroides* in which the biosynthetic pathway was altered such that lycopene was produced as the predominant carotenoid LH2. The HPLC carotenoid analysis of the membrane sample found it to contain 75% lycopene and 20% neurosporene. The details of this sample preparation are presented elsewhere.[31,32] Here the LH2 complex was left in its membrane environment (containing only LH2 complexes and no other pigment−protein species) and was studied only at room temperature (298 K). The LH2 membranes were dissolved in buffer solution (50 mM Tris, pH 8) to an absorption of OD (795 nm) = 0.5 in a 2 mm glass cuvette. The excitation conditions are the same as above.

Experiment. The femtosecond spectrometer employed in these studies is based on an amplified Ti:sapphire laser system, producing ∼100 fs pulses at 795 nm with an average output power of 1 W and a repetition rate of 5 kHz. Part of this light was used directly to excite the B800 Q_y transition. To generate pump pulses at 860 nm, we employed an optical parametric generator/amplifier (Light Conversion, *TOPAS*), and to produce probe pulses spanning the visible spectral region we focused part of the beam into a 5 mm sapphire plate, which yielded a white-light continuum. The relative polarization of the pump and probe pulses was set to the magic angle (54.7°). The pump and probe pulses traveled along different optical paths to the sample; the path length of the former was determined by a computer-controlled optical delay line. The probe pulse was further divided by a 50/50 beam splitter to produce an additional beam that was used as a reference in the pump−probe experiment. This beam also passed through the sample but had no spatial overlap with either the pump or probe beams. The probe and reference beams were detected by photodiodes following dispersion through a single-grating monochromator. The instrument response function was measured by frequency mixing the excitation and probe pulses in a $LiIO_3$ crystal; the cross-correlation signal obtained by this method was fit to a Gaussian function with fwhm ∼140 fs.

Following excitation in the Q_y regions of the BChls with a 100 fs pulse, the visible region (420−650 nm) was probed directly by two techniques. (a) For a fixed pump−probe delay time, the full transient absorption spectrum spanning the visible to near-infrared region was obtained by scanning the detection monochromator. We compensated for group velocity dispersion by properly shifting the delay line for each wavelength. (b) At a fixed detection wavelength, we scanned the delay line to record the transient absorption kinetics of a given species (identified by its characteristic absorption properties).

Calculations. Our calculations are based on the crystal structures of *Rps. acidophila*[4] and *Rs. molischianum*[5] and are performed with the Gaussian 98 program package.[33] Hydrogen atoms were added to the pigment molecules and their position optimized keeping other atoms fixed. The RG in *Rps. acidophila* and the lycopene in *Rs. molischianum* have the same polyene backbone with 11 conjugated CC double bonds. Due to limited resolution, the crystal structures give significantly different CC bond lengths for RG and lycopene. Therefore the Car molecules were further optimized for CC bond lengths holding other Car geometry parameters fixed using density functional theory (DFT) based on the three-parameter Lee−Yang−Parr (B3LYP) functional[34] with the 6-31G** basis set (see Table 1). The atomic level structure of *Rb. sphaeroides* is not known. As a model we used the structure of the *Rps. acidophila* where the RG was replaced by lycopene in such a way that the conjugated π-electron systems of the two Cars were identical. The Car electrostatic environment has been simplified as a charge field of three BChls as in our early work.[16] The point charges of the BChls forming the charge field are obtained via CHelpG population[35] from Hartree−Fock (HF) and/or the single excitation configuration interaction (CIS) wave functions, which can describe the change in the local charge field of the Car upon BChl excitation. The Car S_2 state energies were calculated using the TDDFT method with the 6-31G and 6-31G* bases sets.

Results and Discussion

Room-temperature absorption spectra of the samples are shown in Figure 1. In the near-infrared region all spectra are dominated by characteristic features due to the Q_y bands of

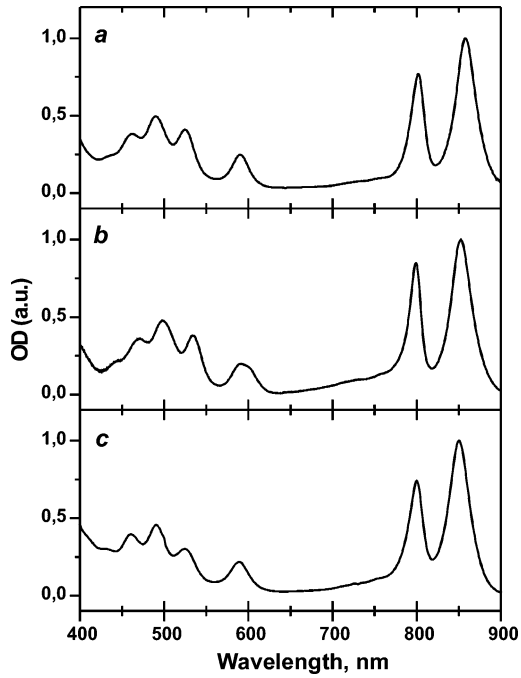

Figure 1. Steady-state absorption spectra of (a) wild-type *Rps. acidophila* LH2, (b) wild-type *Rs. molischianum* LH2, and (c) mutant *Rb. sphaeroides* LH2 (see text for details). All spectra were recorded at 298 K, normalized to absorption maximum.

TABLE 1: CC Bond Lengths (Å) of the Conjugated Region of Carotenoids in Crystal Structures of LH2 Complexes and the Optimized Bond Lengths at B3LYP/6-31G**

			optimization of CC bonds	
C bonds	RG in *Rps. acidophila*	lycopene in *Rs. molischianum*	RG	lycopene
$C_1 = C_2$	1.400	1.349	1.364	1.355
$C_2 - C_3$	1.401	1.457	1.449	1.454
$C_3 = C_4$	1.401	1.352	1.366	1.357
$C_4 - C_5$	1.404	1.483	1.453	1.461
$C_5 = C_6$	1.399	1.347	1.382	1.366
$C_6 - C_7$	1.398	1.467	1.443	1.440
$C_7 = C_8$	1.391	1.338	1.374	1.361
$C_8 - C_9$	1.397	1.485	1.446	1.448
$C_9 = C_{10}$	1.398	1.339	1.383	1.375
$C_{10} - C_{11}$	1.393	1.457	1.434	1.436
$C_{11} = C_{12}$	1.405	1.327	1.376	1.369
$C_{12} - C_{13}$	1.391	1.467	1.434	1.436
$C_{13} = C_{14}$	1.393	1.362	1.382	1.368
$C_{14} - C_{15}$	1.400	1.493	1.447	1.456
$C_{15} = C_{16}$	1.406	1.349	1.372	1.360
$C_{16} - C_{17}$	1.401	1.465	1.438	1.442
$C_{17} = C_{18}$	1.403	1.345	1.379	1.363
$C_{18} - C_{19}$	1.397	1.483	1.450	1.468
$C_{19} = C_{20}$	1.396	1.345	1.367	1.353
$C_{20} - C_{21}$	1.388	1.462	1.450	1.456
$C_{21} = C_{22}$	1.388	1.353	1.363	1.352

BChl-a. While the position of the B800 band remains at 800 nm for all three LH2 species, the position of the B850 band varies from species to species, peaking at 858 nm for *Rps. acidophila*, at 853 nm for *Rs. molischianum*, and at 850 nm for *Rb. sphaeroides* mutant. The significant difference between structures of LH2 complexes from *Rps. acidophila* and *Rs. molischianum* is reflected in a splitting of the Q_x band of BChl-a in the case of *Rs. molischianum*, while similarity between absorption spectra of *Rps. acidophila* and *Rb. sphaeroides* points to much closer structures, as suggested earlier by cryoelectron microscopy.[36] In the 450−550 nm region, a typical three-peak absorption feature due to the S_2 state of carotenoid dominates

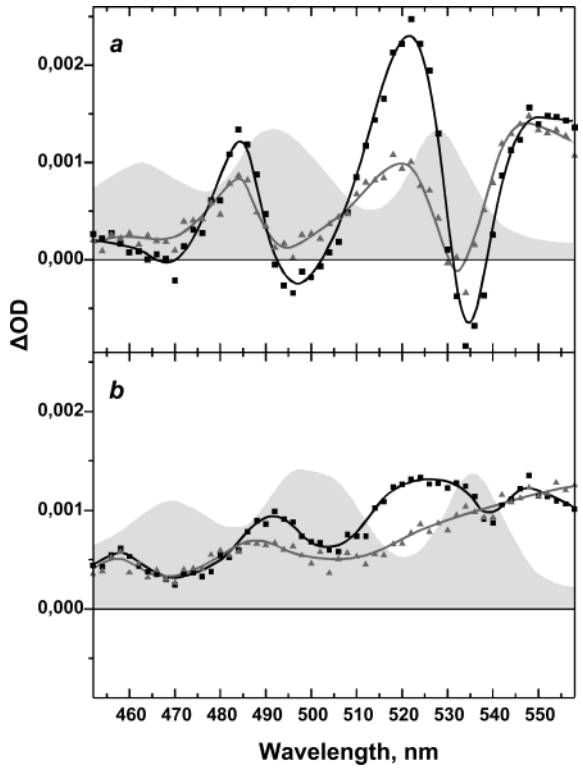

Figure 2. Transient absorption spectra in the carotenoid region following excitation of B800 BChl at 795 nm. $T = 77$ K. Wild-type LH2 from (a) *Rps. acidophila* and (b) *Rs. molischianum*. Symbols represent raw data obtained at a time delay of 0.3 ps (squares) and 10 ps (triangles). The curves are the result of applied smoothing functions. The underlying filled gray regions are the corresponding steady-state absorption spectra (a.u.) at $T = 77$ K.

the absorption spectrum. In all LH2 species, the carotenoid S_2 state is significantly red-shifted from its position in solution as a result of interaction with protein. The lowest energy band of the S_2 state peaks at 525 nm for LH2 from *Rps. acidophila* containing rhodopin glucoside, indicating a shift of 900 cm^{-1} as compared with the value in methanol solution.[37] A significantly larger shift of 1200 cm^{-1} is observed for lycopene in LH2 from *Rs. molischianum*, where the 0−0 band is located at 535 nm, again underlining differences in LH2 structures of these two organisms. We point out that here and in the following if we give a value for a spectral shift then we always mean the shift of the 0−0 band. The shift of the other vibrational bands is not significantly different. In the case of *Rb. sphaeroides* mutant containing lycopene, the lowest transition of the S_2 state is located at 526 nm. The corresponding protein-induced shift is 900 cm^{-1}, which is less than the value observed for spheroidene in the wild-type LH2 of *Rb. sphaeroides*,[37] indicating a slightly weaker interaction of lycopene with the protein environment in the binding pocket. It is also necessary to mention that the *Rb. sphaeroides* mutant contains a fraction (∼20%) of neurosporene.[31]

The difference between LH2 complexes from *Rps. acidophila* and *Rs. molischianum* is further demonstrated by transient signals in the carotenoid region that were ascribed to a band shift of carotenoid absorption induced by local electric field generated by excited BChl-a molecules.[26] In Figure 2 are shown low temperature (77 K) transient absorption spectra recorded at 0.3 and 10 ps after excitation of B800 at 795 nm. The two recording times correspond to almost pure excitation of B800 or B850, respectively. In the case of *Rps. acidophila*, the 0.3 ps transient absorption spectrum exhibits the characteristic

TABLE 2: Calculated S_2 Energies of Carotenoids in Different Charge Fields Consisting of the Protomer Unit[a]

	RG in *Rps. acidophila*						Lycopene in *Rs. molischianum*					
	GS			S_1 (B800)			GS			S_1 (B800)		
basis sets	eV	nm	f	eV	nm	f	eV	nm	f	eV	nm	f
6-31G	2.077	596.8	3.6282	2.087	594.1 (−2.7)	3.7156	2.221	558.3	4.0054	2.221	558.2 (−0.1)	4.0060
6-31G*	2.047	605.8	3.6331	2.060	601.8 (−4.0)	3.7564	2.191	566.0	3.9779	2.191	565.9 (−0.1)	3.9788

[a] GS denotes the charge field of the ground state where the point charges are obtained from HF wave functions. In the S_1 (B800) case, B800 is in the excited-state S_1 and the corresponding charges are generated from CIS wave functions. Two B850 BChl molecules are still in the ground state. The values in parentheses refer to the wavelength shifts.

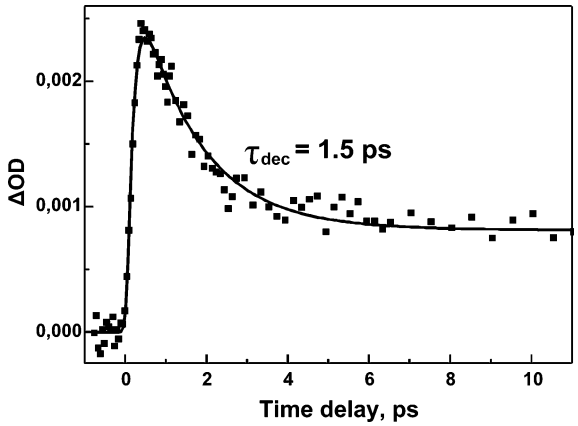

Figure 3. Transient absorption kinetics recorded at 522 nm following excitation of B800 BChl at 795 nm. $T = 77$ K. Wild-type *Rps. acidophila* LH2. Symbols represent raw data; the curve is the result of a multiexponential function convoluted with a Gaussian response function (fwhm = 140 fs). The principle decay component (60%) has a time constant of 1.5 ± 0.1 ps.

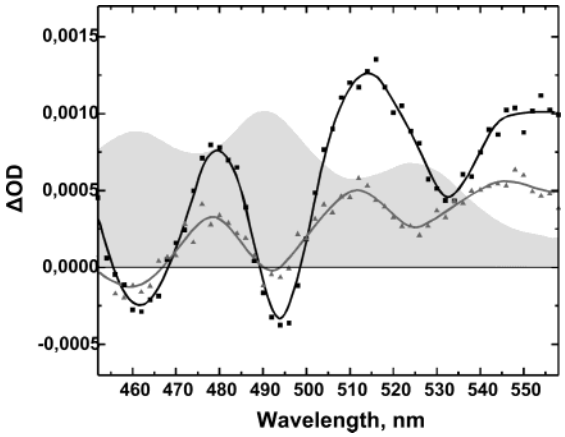

Figure 4. Transient absorption spectra in the carotenoid region following excitation of B800 BChl at 795 nm. $T = 298$ K. Mutant *Rb. sphaeroides* LH2. Symbols represent raw data obtained at a time delay of 0.3 ps (squares) and 10 ps (triangles). The curves are the result of applied smoothing functions. The underlying filled gray region is the corresponding steady-state absorption spectra (a.u.) at $T = 298$ K.

band-shift pattern, which can be simulated by a 3 nm blue shift of the steady-state absorption spectrum. To reproduce the spectrum precisely, a nonuniform background due to weak BChl-a excited-state absorption must be taken into account. A similar, but weaker carotenoid response is observed in the 10 ps transient absorption spectrum. The change of the carotenoid response due to B800−B850 energy transfer is clearly seen in Figure 3, where decay kinetics recorded at 522 nm follow the known B800−B850 transfer rate at 77 K.[8] On the other hand, the response of lycopene to excitation of B800 in LH2 from *Rs. molischianum* is significantly weaker, as the 0.3 ps transient absorption spectrum is dominated by a positive signal due to BChl-a excited state absorption that bears only a weak wavy pattern due to the lycopene band shift. Within the first few picoseconds, this signal decays to form a rather featureless positive excited state absorption, suggesting that when the excitation resides at B850 BChl-a molecules, no band shift is produced. It was carefully checked that, despite this dramatic difference in carotenoid response, the magnitude of B850 bleaching at 2 ps is identical for both LH2 species. Thus, the origin of the difference lies solely in structural variance of these two complexes.

We have performed the same experiments for LH2 complexes from a *Rb. sphaeroides* mutant in which the naturally occurring carotenoid spheroidene is replaced by lycopene. As shown in Figure 4, room-temperature transient absorption spectra recorded at 0.3 and 10 ps exhibit a clear pattern characteristic of lycopene band shift, having magnitude comparable to that observed for LH2 from *Rps. acidophila* at 77 K. The fact that the same carotenoid lycopene in two different species, *Rs. molischianum* and *Rb. sphaeroides*, has such a different response to the B800 excitation strongly suggests that the Car band shift is very sensitive to the local environment of the molecule. If we compare the two known structures, *Rps. acidophila* and *Rs. molischianum*, which lead to the different Car band shifts, then indeed, the B800 molecules in the two species are oriented in a rather different way. This means that the local field changes in two structures upon B800 excitation are different. We do not know the exact structure of *Rb. sphaeroides*, but existing indirect evidence[36] suggests that it is very similar to the structure of *Rps. acidophila*. The strong Car band shift observed here gives additional support to that view.

To verify our conclusions, we have carried out a series of calculations of Car responses to the changes in the local field upon excitation of the B800. Table 2 summarizes the calculations of the S_2 energies for Car in two LH2 complexes with known structures. In *Rps. acidophila* the calculations indicate the RG S_2 energy shifts to the blue ($3 \sim 4$ nm). This is consistent with the previous CASSCF calculations[16] and justifies the use of the computationally cheaper TDDFT method in the current work. Calculations do not give any appreciable S_2 band shift for the lycopene in *Rs. molischianum*. These findings are in good qualitative and even quantitative agreement with the experimental results. When the calculations are performed with the *Rps. acidophila* structure with RG replaced by lycopene, the calculations again yield a blue shift of the S_2 band (Table 3). This proves that the differences of the arrangement of the pigment molecules and not the type of the Car are responsible of the differences in Car band shifts.

In the following we will use the above results for estimating the static local field strength near the Car molecule in the LH2 protein. It has to be pointed out that the local field in a complex protein environment is most likely not constant. Furthermore,

TABLE 3: Calculated S_2 Energy of Carotenoid Lycopene in the Local Electrostatic Environment of *Rps. acidophila* Complex[a]

	GS			S_1 (B800)		
basis sets	eV	nm	f	eV	nm	f
6-31G	2.072	598.4	3.6026	2.081	595.7 (−2.7)	3.6821
6-31G*	2.044	606.5	3.6284	2.058	602.4 (−4.1)	3.7528

[a] For the notation see Table 2.

it has been shown that the details of the local field may significantly affect the Stark shift of a Car molecule.[38] Using the crystal structure of LH2 it would in principle be possible to use quantum chemistry calculations to evaluate the local field of the Car based on the nearby amino acid residues. Such an analyses would go beyond the scope of the current article. Here we assume a homogeneous local field around the Car molecule. The Stark shift of the electronic transition frequency of a molecule can be expressed as[39]

$$\Delta\nu = -h^{-1}\left(\Delta\mu\mathbf{F}_d + \Delta\alpha\mathbf{F}\mathbf{F}_d + \frac{1}{2}\Delta\alpha\mathbf{F}_d\mathbf{F}_d\right) \qquad (1)$$

where $\Delta\mu$ and $\Delta\alpha$ are the change of the dipole moment and polarizabilty upon the electronic transition (in our case Car S_0-S_2 transition), $\mathbf{F}$ is the local electric field and $\mathbf{F}_d$ is the Stark field at the place of the molecule. In our case $\mathbf{F}_d$ corresponds to the change of the local field upon B800 excitation.

In the following we will estimate the strength of the static local field near Car in LH2. The magnitude of Car $\Delta\mu$ and $\Delta\alpha$ depends to some extent on the environment. Based on the Stark spectroscopy studies[40] we use $\Delta\mu = 4$ D and $\Delta\alpha = 1500$ Å^3 for lycopene. We are not aware of any studies that reveal the orientation of $\Delta\mu$ and $\Delta\alpha$ for RG and lycopene. Intuitively it is highly likely that they both are oriented along the axes of the molecule (rigorously $\Delta\alpha$ is a tensor).

Now we need to evaluate the change of the local electric field upon B800 excitation $-\mathbf{F}_d$. Both Stark spectroscopy measurements[41] and quantum chemistry calculations[16] have shown that the difference of the electrical dipole of the BChl molecule in the ground state and the S1 state, $\Delta\mu$, is oriented parallel to the Q_y transition dipole moment. Multilevel modeling of the TDDFT calculations of BChl in electric field[42] gave $\Delta\mu = 0.2$ D for the BChl Q_y transition. Experimental Stark spectroscopy studies[39,43] have given somewhat higher values for $\Delta\mu$ for B800 since local field induces additional $\Delta\mu$ via polarizability change $\Delta\alpha$.[39] In the following we are using the experimental value of $\Delta\mu \approx 1$ D for B800. Part of the Car is very close to the B800. It has even been suggested that a weak C−H···O hydrogen bond may occur between the Car and B800 in *Rps. acidophila*.[44] For the current order-of-magnitude estimate we use 10 Å for an effective distance between Car and B800, which gives 0.3 MV/cm for the field strength change. The last term in eq 1 leads to the red shift of about 4 cm^{-1} for $\Delta\alpha = 1500$ Å^3. The first term shifts the spectrum by 20 cm^{-1}. This shift may be either to the red or blue depending on the orientation of the $\Delta\mu$ in respect to the change of the electric field. To obtain the experimentally observed blue shift of about 120 cm^{-1} we can evaluate from the second term in eq 1 the local field $\mathbf{F} = 4$ or 6 MV/cm, depending on the direction of the $\Delta\mu$ in the first term. Similar local field strengths in proteins have been measured using Car response to the transmembrane potential[45−47] and other techniques.[48] In our case the direction of the local field $\mathbf{F}$ has to be opposite to the change of the field induced by the BChl excitation $\mathbf{F}_d$. We can see that the second term of eq 1 dominates the overall effect of the ultrafast band shift. We can also evaluate how large is a portion of the red shift of the Car band in protein due to the local field. Since $\mathbf{F}$ and $\mathbf{F}_d$ have opposite directions, we can conclude that in the case of a 6 MV/cm field $\Delta\mu$ induces a blue shift of about 400 cm^{-1}, whereas the $\Delta\alpha$ leads to a red shift of 1500 cm^{-1}. The overall shift would be 1100 cm^{-1}. Using similar argumentation we would conclude that the field 4 MV/cm induces the red shift via both $\Delta\mu$ and $\Delta\alpha$ with an overall shift 930 cm^{-1}. These numbers are very close to the observed shifts of the Car absorption spectra if one compares the Car in light harvesting complexes with Car in solution (see above). Admittedly the above estimates have rather large error bars (∼20−30%), but we can still conclude that the major part of the Car spectral shift in light harvesting complexes compared

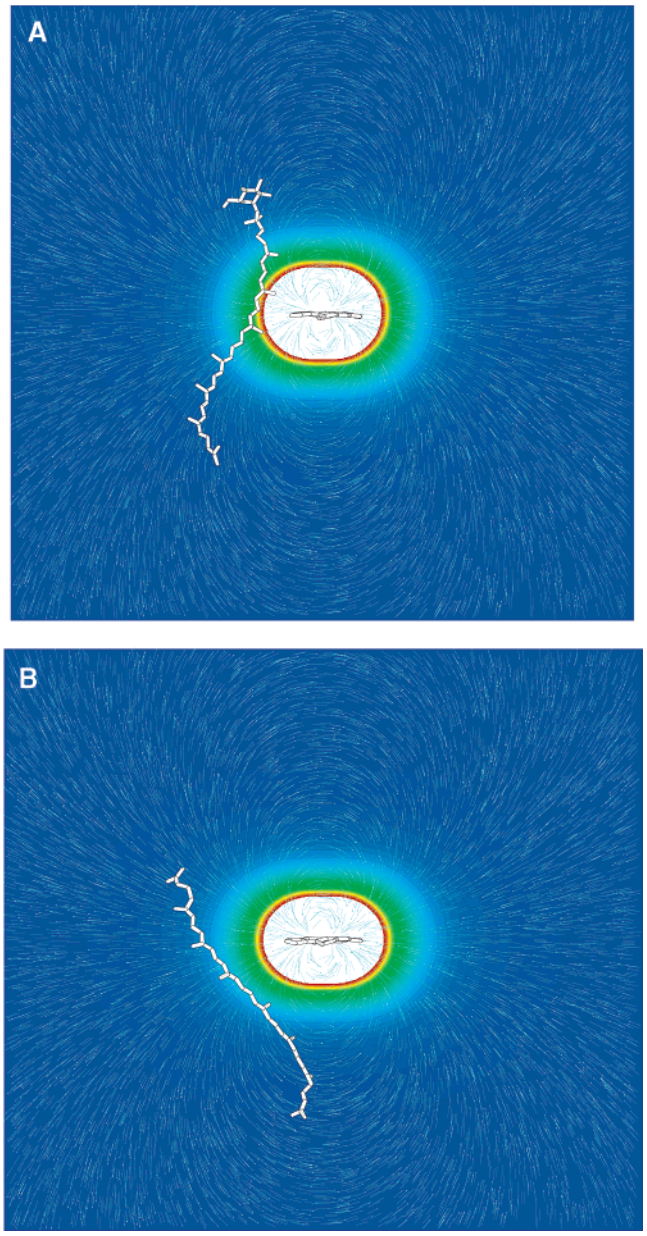

Figure 5. B800 and Car molecules together with the field induced by the $\Delta\mu$ of B800 for *Rps. acidophila* (A) and *Rs. molischianum* (B). The color coding indicates the strength of the field (red strong, blue weak), whereas the thin lines show the direction of the field. It can be seen that in *Rps. acidophila* the field is parallel to the Car molecule for a major part of the Car, whereas in *Rs. molischianum* only a very short part of the Car quite far from B800 is parallel to the field.

to solution comes from the local electric field rather than from dispersion forces (London forces). One of the important residues forming the field apparently is the βArg-10. Mutating this residue shifts both the B800 and the Car absorption bands.[49,50] Furthermore, the mutation drastically reduces the electrochromic carotenoid band shift in LH2.[51] Interestingly, this residue is present in *Rps. acidophila* and *Rb. sphaeroides*, both having a strong ultrafast band shift, but not in *Rs. molischianum*.

Finally, in Figure 5 we show the field of the BChl $\Delta\mu$ together with corresponding B800 and Car molecules in two different structures. From the figure it can be noted that in the case of *Rs. molischianum* most of the π-conjugated system is perpendicular to the field, whereas in *Rps. acidophila* a significant part of the Car is parallel to the field. Consequently the differences in Car response in these two systems can be qualitatively explained by the structural arrangement of the pigment molecules.

Conclusions

The ultrafast Car band shift upon BChl excitation in LH2 is a result of a change in local electric field. TDDFT calculations strongly suggest that the mutual orientation of pigment molecules in LH2 determines the extent of the band shift. The estimated strength of the local field near Car depends on the direction of the Car $\Delta\mu$ and is 4 or 6 MV/cm. The major part of the additional red shift of the Car in LH2, compared to the Car in solution, is due to the environment-induced local field.

Acknowledgment. This work was supported by the Swedish Research Council (Lund) and BBSRC (Glasgow).

References and Notes

(1) Cogdell, R. J.; Frank, H. A. *Biochim. Biophys. Acta* **1987**, *895*, 63.
(2) Polívka, T.; Sundström, V *Chem. Rev.* **2004**, *104*, 2021.
(3) Lang, H. P.; Hunter, C. N. *Biochem. J.* **1994**, *298*, 197.
(4) McDermott, G.; Prince, S. M.; Freer, A. A.; Hawthornthwaite-Lawless, A. M.; Papiz, M. Z.; Cogdell, R. J.; Isaacs, N. W. 1995 *Nature* **1995**, *374*, 517.
(5) Koepke, J.; Hu, X.; Muenke, C.; Schulten, K.; Michel, H. *Structure* **1996**, *4*, 581.
(6) Shreve, A. P.; Trautman, J. K.; Frank, H. A.; Owens, T. G.; Albrecht, A. C. *Biochim. Biophys. Acta* **1991**, *1058*, 280.
(7) Hess, S.; Feldchtein, F.; Babin, A.; Nurgaleev, I.; Pullerits, T.; Sergeev, A.; Sundström, V. *Chem. Phys. Lett.* **1993**, *216*, 247.
(8) Pullerits, T.; Hess, S.; Herek, J. L.; Sundström V. *J. Phys. Chem.* **1997**, *101*, 10560.
(9) Herek, J. L.; Fraser, N.; Pullerits, T.; Martinsson, P.; Polívka, T.; Scheer, H.; Cogdell, R. J.; Sundström, V. 2000 *Biophys. J.* **78**, 2590.
(10) Scholes, G. D.; Fleming, G. R. *J. Phys. Chem. B* **2000**, *104*, 1854.
(11) Mukai, K.; Abe, S.; Sumi, H. *J. Phys. Chem. B* **1999**, *103*, 6096.
(12) Kimura, A.; Kakitani, T. *J. Phys. Chem. B* **2003**, *107*, 7932.
(13) Tavan, P.; Schulten, K. *J. Chem. Phys.* **1986**, *85*, 6602.
(14) Sashima, T.; Nagae, H.; Kuki, M.; Koyama, Y. *Chem. Phys. Lett.* **1999**, *299*, 187.
(15) Hsu, C.-P.; Walla, P. J.; Head-Gordon, M.; Fleming, G. R. *J. Phys Chem. B* **2001**, *105*, 11016.
(16) He, Z.; Sundström, V.; Pullerits, T. *Chem. Phys. Lett*. **2001**, *334*, 159.
(17) Gradinaru, C. C.; Kennis, J. T. M.; Papagiannakis, E.; van Stokkum, I. H. M.; Cogdell, R. J.; Fleming, G. R.; Niederman, R. A.; van Grondelle, R. *Proc. Natl. Acad. Sci. U.S.A* **2001**, *98*, 2364.
(18) Sundström, V.; Pullerits, T.; van Grondelle, R. *J. Phys. Chem. B* **1999**, *103*, 2327.
(19) Herek, J. L.; Wohlleben, W.; Cogdell, R. J.; Zeidler, D.; Motzkus, M. *Nature* **2002**, *417*, 533.
(20) Förster, T. In *Modern Quantum Chemistry*; Sinanoglu, O., Ed.; Academic Press: New York, 1965; p 93.
(21) Nagae, H.; Kakitani, T.; Katoh, T.; Mimuro, M. *J. Chem. Phys.* **1993**, *98*, 8012.
(22) Krueger, B. P.; Scholes, G. D.; Fleming, G. R. *J. Phys. Chem. B* **1998**, *102*, 5378.
(23) Zhang, J.-P.; Fujii, R.; Qian, P.; Inaba, T.; Mizoguchi, T.; Koyama, Y.; Onaka, K.; Watanabe, Y. *J. Phys. Chem. B* **2000**, *104*, 3683.
(24) Zigmantas, D.; Hiller, R. G.; Sundström, V.; Polívka, T. *Proc. Natl. Acad. Sci. U.S.A.* **2002**, *99*, 16760.
(25) Papiz, M. Z.; Prince, S. M.; Howard, T.; Cogdell, R. J.; Isaacs, N. W. *J. Mol. Biol.* **2003**, *326*, 1523.
(26) Herek, J. L.; Polívka, T.; Pullerits, T.; Fowler, G. J. S.; Hunter, C. N.; Sundström, V. *Biochemistry* **1998**, *37*, 7057.
(27) Gottfried, D. S.; Steffen, M. A.; Boxer, S. G. *Science* **1991**, *251*, 662.
(28) Fleischman, D. E.; Clayton, R. K. *Photochem. Photobiol.* **1968**, *8*, 287.
(29) Gosztola, D.; Yamada, H.; Wasielewski, M. R. *J. Am. Chem. Soc.* **1995**, *117*, 2041.
(30) Fraser, N. J.; Dominy, P. J.; Ücker, B.; Siminin, I.; Scheer, H.; Cogdell, R. J. *Biochemistry* **1999**, *38*, 9684.
(31) Billsten, H. H.; Herek, J. L.; Garcia-Asua, G.; Hashøj, L.; Polívka, T.; Hunter, C. N.; Sundström, V. *Biochemistry* **2002**, *41*, 4127.
(32) Garcia-Asua, G.; Cogdell, R. J.; Hunter, C. N. *Mol. Microbiol.* **2002**, *44*, 233.
(33) Frisch, M. J.; Trucks, G. W.; Schlegel, H. B.; Scuseria, G. E.; Robb, M. A.; Cheeseman, J. R.; Zakrzewski, V. G.; Montgomery, Jr., J. A.; Stratmann, R. E.; Burant, J. C.; Dapprich, S.; Millam, J. M.; Daniels, A. D.; Kudin, K. N.; Strain, M. C.; Farkas, O.; Tomasi, J.; Barone, V.; Cossi, M.; Cammi, R.; Mennucci, B.; Pomelli, C.; Adamo, C.; Clifford, S.; Ochterski, J.; Petersson, G. A.; Ayala, P. Y.; Cui, Q.; Morokuma, K.; Malick, D. K.; Rabuck, A. D.; Raghavachari, K.; Foresman, J. B.; Cioslowski, J.; Ortiz, J. V.; Stefanov, B. B.; Liu, G.; Liashenko, A.; Piskorz, P.; Komaromi, I.; Gomperts, R.; Martin, R. L.; Fox, D. J.; Keith, T.; Al-Laham, M. A.; Peng, C. Y.; Nanayakkara, A.; Gonzalez, C.; Challacombe, M.; Gill, P. M. W.; Johnson, B.; Chen, W.; Wong, M. W.; Andres, J. L.; Gonzalez, C.; Head-Gordon, M.; Replogle, E. S.; Pople, J. A. **1998**, *Gaussian 98*, Gaussian, Inc.: Pittsburgh, PA.
(34) Becke, A. D. *J. Chem. Phys.* **1993**, *98*, 5648.
(35) Breneman, C. M.; Wiberg, K. B. *J. Comput. Chem.* **1990**, *11*, 361.
(36) Walz, T.; Jamieson, S. J.; Bowers, C. M.; Bullough, P. A.; Hunter, C. N. *J. Mol. Biol.* **1998**, *282*, 833.
(37) Polívka, T.; Zigmantas, D.; Herek, J. L.; He, Z.; Pascher, T.; Pullerits, T.; Cogdell, R. J.; Frank, H. A.; Sundström, V. *J. Phys. Chem. B* **2002**, *106*, 11016.
(38) Kakitani, T.; Honig, B.; Crofts, A. R. *Biophys. J.* **1982**, *39*, 57.
(39) Rätsep, M.; Wu, H.-M.; Hayes, J. M.; Blankenship, R. E.; Cogdell, R. J.; Small, G. J. *J. Phys. Chem. B* **1998**, *102*, 4035.
(40) Krawczyk, S.; Olszowka, D. *Chem. Phys.* **2001**, *265*, 335.
(41) Beekman, L. M. P.; Steffen, M.; van Stokkum, I. H. M.; Olsen, J. D.; Hunter, C. N.; Boxer, S. G.; van Grondelle, R. *J. Phys. Chem. B* **1997**, *101*, 7284.
(42) Kjellberg, P.; He, Z.; Pullerits, T. *J. Phys. Chem. B* **2003**, *107*, 13737.
(43) Beekman, L. M. P.; Frese, R. N.; Fowler, G. J. S.; Picorel, R.; Cogdell, R. J.; van Stokkum, I. H. M.; Hunter, C. N.; van Grondelle, R. *J. Phys. Chem. B* **1997**, *101*, 7293.
(44) He, Z.; Sundström, V.; Pullerits, T. *FEBS Lett.* **2001**, *496*, 36.
(45) De Grooth, B. G.; Amesz, J. *Biochim. Biophys. Acta* **1977**, *462*, 247.
(46) Holmes, B. G.; Crofts, A. R. *Biochim. Biophys. Acta* **1977**, *459*, 492.
(47) Symons, M.; Swysen, C.; Sybesma, C. *Biochim. Biophys. Acta* **1977**, *462*, 706.
(48) Laberge, M.; Vanderkooi, J. M.; Sharp, K. A. *J. Phys. Chem.* **1996**, *100*, 10793.
(49) Fowler, G. J. S.; Hess, S.; Pullerits, T.; Sundström, V.; Hunter, C. N. *Biochemistry* **1997**, *36*, 11282.
(50) Gall, A.; Sturgis, J. D.; Fowler, G. J. S.; Hunter, C. N.; Robert, B. *Biochemistry* **1997**, *36*, 16282.
(51) Crielaard, W.; Visschers, R. W.; Fowler, G. J. S.; van Grondelle, R.; Hellingwerf, K. J.; Hunter, C. N. *Biochim. Biophys. Acta* **1994**, *1183*, 473.